Crystal Structure of the Emptied Clathrate Form (δ_e Form) of Syndiotactic Polystyrene

Claudio De Rosa,* Gaetano Guerra,† Vittorio Petraccone, and Beniamino Pirozzi

Dipartimento di Chimica, Università di Napoli Federico II, Via Mezzocannone 4, I-80134 Naples, Italy, and Dipartimento di Chimica, Università di Salerno, I-84081 Baronissi (SA), Italy

Received January 22, 1997; Revised Manuscript Received April 21, 1997[⊗]

ABSTRACT: The crystal structure of the emptied clathrate form (δ_e form) of syndiotactic polystyrene, obtained by removing the guest molecules from different clathrate δ forms, is presented. Chains in s(2/1)2 helical conformation are packed in the monoclinic unit cell with axes $a = 17.4$ Å, $b = 11.85$ Å, $c = 7.70$ Å, and $\gamma = 117°$ according to the space group $P2_1/a$. The crystalline density of the emptied clathrate form (0.977 g/cm^3) is lower than that of the amorphous phase (1.055 g/cm^3). The differences between the structures of the emptied clathrate form and clathrate δ forms are discussed by the analysis of X-ray diffraction patterns and packing energy calculations.

Introduction

Syndiotactic polystyrene (s-PS) presents a very complex polymorphic behavior.[1−6] Four different crystalline forms have been described so far. Following the nomenclature proposed in ref 2, the crystalline α and β forms are characterized by chains in the *trans* planar conformation, whereas the crystalline γ and δ forms contain chains in the s(2/1)2 helical conformation. The term "δ form" has been used to indicate different clathrate structures where helices of s-PS (the host) form a crystal lattice containing spaces in which molecules of a second chemical species (the guest) are located. For these clathrate structures, the intensities and the precise locations of the reflections in the X-ray diffraction patterns change with the kind and the amount of the included guest molecules.[1,2]

The crystal structures of α[3,7,8] and β[4,9] forms have been determined. Both α and β forms can exist in different modifications having different degrees of structural order, so that two limiting disordered modifications (α′ and β') and two limiting ordered modifications (α″ and β'') have been described.[2−4,8] Besides the four crystalline forms, two mesomorphic modifications of s-PS, containing chains in the *trans* planar and the s(2/1)2 helical conformations, have been also described.[10−13]

The clathrate δ form can be obtained by sorption of suitable compounds (e.g., methylene chloride, 1,2-dichloroethane, toluene, etc.) in amorphous s-PS samples as well as in semicrystalline s-PS samples being in the α or γ form. The crystal structures of clathrate δ forms including molecules of toluene[14] and iodine[15] have been described.

An emptied clathrate form of s-PS (δ_e form), which corresponds to a pure helical form of s-PS free from the guest molecules, can be obtained by suitable solvent extraction procedures on samples in the clathrate δ form.[13,16] Samples of s-PS in the emptied clathrate form rapidly absorb molecules of suitable organic substances and transform into the clathrate δ form. The capability of emptied clathrate form samples of s-PS to selectively absorb specific organic substances can be used to separate solvent mixtures or purify streams from traces of specific organic substances.[16] The X-ray diffraction patterns of unoriented samples in the emptied clathrate form as well as their changes induced by thermal treatments have been recently described in ref 13.

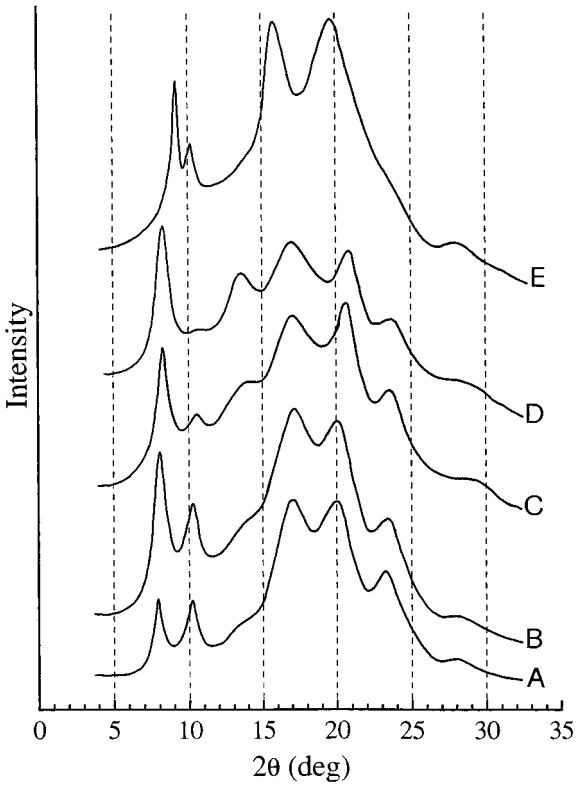

Figure 1. X-ray powder diffraction profiles of clathrate δ forms of s-PS including (A) 14, (B) 8 and (C) 5.7 wt % toluene, of the emptied clathrate δ form including less then 1 wt % toluene (D), and of the γ form (E).

It is worth noting that the emptied clathrate form of s-PS (δ_e form) is different from the γ form which is obtained by annealing the clathrate δ form or the emptied clathrate form, for instance, at ≈130 °C.[13] Both forms include only chains of s-PS in the helical s(2/1)2 conformation, without guest molecules, and therefore, two different pure helical forms, free from guest molecules (δ_e and γ forms), exist for s-PS. In this paper the crystal structure of the emptied clathrate δ form (δ_e form) is presented.

† Università di Salerno.

[⊗] Abstract published in *Advance ACS Abstracts,* June 1, 1997.

S0024-9297(97)00061-2 CCC: $14.00

Table 1. Calculated Structure Factors, F_c, of Reflections Observed in the Region of 2θ between 7° and 14° for the Model of the Crystal Structure of the Clathrate δ Form Including Toluene Proposed by Chatani et al.[14] (a = 17.58 Å, b = 13.26 Å, c = 7.71 Å, γ = 121.2°, space group $P2_1/a$) for Different Values of the Occupancy Factor (o.f.) of the Atoms of Toluene[a]

		F_c					
hkl	2θ (deg)	o.f. = 1	o.f. = 0.8	o.f. = 0.6	o.f. = 0.4	o.f. = 0.2	o.f. = 0
010	7.79	56	69	82	95	108	121
$\bar{2}10$	10.21	56	46	35	24	14	3
200	11.77	9	1	6	13	21	28
101	12.90	3	15	28	40	53	65
$\bar{1}11$	13.41	36	49	62	75	89	101
$\bar{2}20$	13.86	21	30	40	49	58	67
011	13.89	2	2	1	1	0	0

[a] The calculations were performed with the thermal factor and the fractional coordinates reported by Chatani et al.[14] The calculated Bragg angles 2θ are also shown.

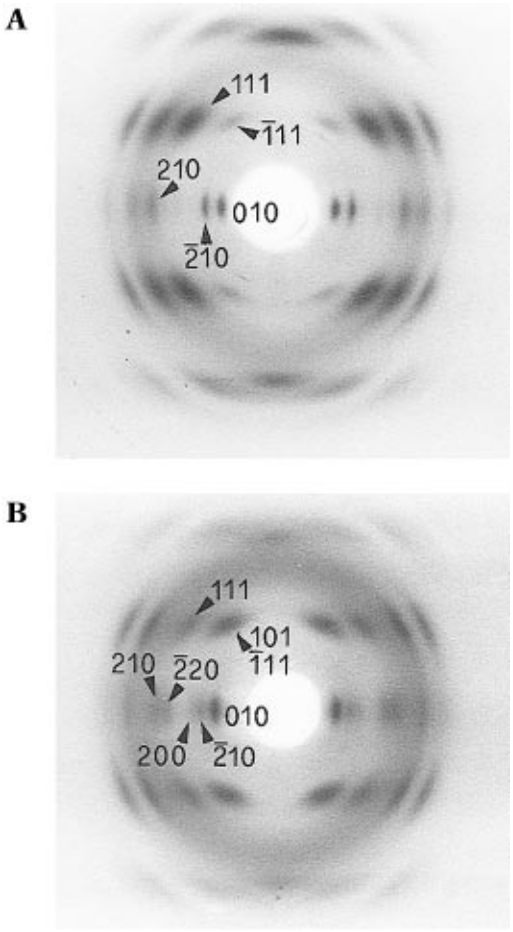

Figure 2. X-ray fiber diffraction patterns of the clathrate δ form including toluene (A) and the corresponding emptied clathrate δ form (B). The indices of the most important reflections are also shown.

Experimental Section

The s-PS was synthesized in our laboratories using a homogeneous catalyst consisting of $CpTiCl_3$ (Cp = cyclopentadienyl) and methylalumoxane (MAO) in toluene, according to the method described in ref 17. The polymer fraction insoluble in acetone is 92%. The intrinsic viscosity of the fraction insoluble in acetone, determined in tetrahydronaphthalene at 135 °C with an Ubbelohde viscosimeter, is 0.60 dL g^{-1}.

The samples in the clathrate δ forms were obtained with different procedures: the clathrate δ form with 14 wt % toluene was obtained by immersion of a sample in the α form in toluene for 48 h at 60 °C; the clathrate δ forms with 8 and

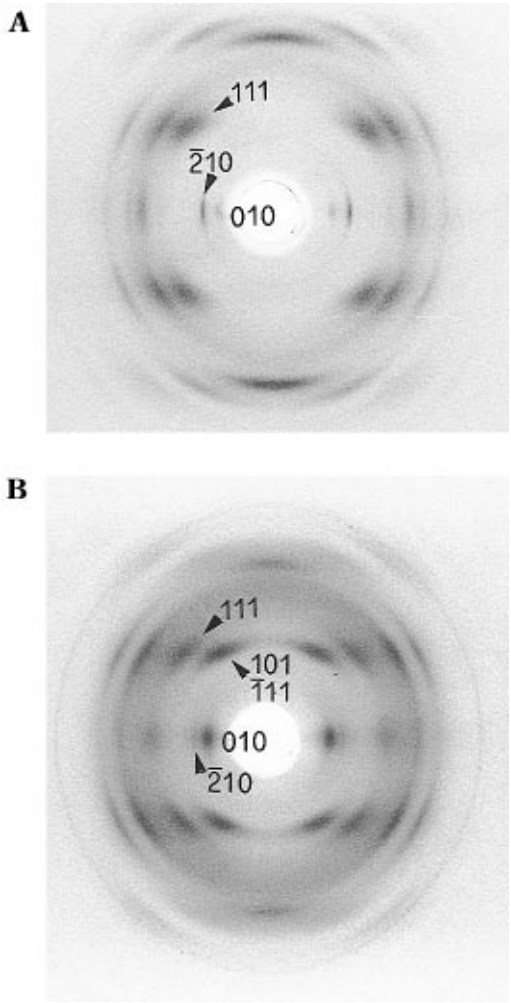

Figure 3. X-ray fiber diffraction patterns of the clathrate δ form including chloroform (A) and the corresponding emptied clathrate δ form (B). The indices of the most important reflections are also shown. (A) The indices of the reflections are given in the assumption that the crystal structure of the clathrate δ form containing chloroform is similar to that of the clathrate δ form containing toluene.[14]

5.7 wt % toluene and the emptied δ form (including less than 1 wt % toluene) were obtained by extractions of samples in clathrate δ forms with boiling acetone for 1, 3, and 7 h, respectively; the sample in γ form was obtained by annealing clathrate δ forms at 130 °C. The extraction procedures were performed with Kumagawa extractors. The content of toluene in the samples was evaluated by thermogravimetric analysis.

Oriented fibers in the clathrate δ forms including toluene or chloroform were obtained by exposing fibers in the α form to vapors of toluene or chloroform. Fibers in the α form were obtained by stretching extruded samples of s-PS at 130 °C. The oriented fibers of the corresponding emptied clathrate forms were obtained by extractions of the fibers in clathrate δ forms with boiling acetone for 7 h.

Wide-angle X-ray powder diffraction patterns were obtained with nickel-filtered Cu Kα radiation with an automatic Philips diffractometer. The X-ray fiber diffraction patterns were obtained with nickel-filtered Cu Kα radiation by using a photographic cylindrical camera.

The thermogravimetric analyses were carried out with a Mettler TG50 Thermobalance in a flowing-nitrogen atmosphere at a heating rate of 10 K/min.

Calculated X-ray diffraction intensities were obtained from the calculated structure factors as $I_c = |F_c|^2 \cdot M \cdot LP$, where M is the multiplicity factor and LP is the Lorentz polarization factor for X-ray fiber diffraction: $LP = (1 + \cos^2 2\theta)/(\sin^2 2\theta - \zeta^2)^{1/2}$. A thermal factor of B = 8 Å^2 and atomic scattering factors from ref 18 were used.

Table 2. Diffraction Angles 2θ, Bragg Distances *d*, Reciprocal Coordinates ξ and ζ, and Intensities *I* of the Reflections Observed on the Layer Lines *l* in the X-ray Fiber Diffraction Pattern of the Emptied Clathrate δ Form of Figure 2B

2θ (deg)	*d* (Å)	ξ (Å^{-1})	ζ (Å^{-1})	*l*	*I*[a]
8.37	10.56	0.095	0	0	vs
10.6	8.34	0.120	0	0	vw
11.5	7.96	0.130	0	0	vw
15.0	5.91	0.169	0	0	w
17.0	5.22	0.192	0	0	w
20.75	4.28	0.234	0	0	w
13.35	6.63	0.077	0.130	1	vs
16.8	5.28	0.138	0.130	1	ms
20.7	4.30	0.193	0.130	1	s
23.5	3.78	0.230	0.130	1	s
23.4	3.80	0	0.260	2	ne
24.8	3.58	0.102	0.260	2	m
28.7	3.10	0.190	0.260	2	mw
33.3	2.70	0.266	0.260	2	vw

[a] vs = very strong, s = strong, ms = medium strong, m = medium, mw = medium weak, w = weak, vw = very weak, ne = not evaluated.

Results and Discussion

X-ray Diffraction Patterns of Unoriented Samples. The X-ray diffraction patterns of s-PS unoriented samples in the clathrate δ form containing variable amounts of toluene and in the γ form are reported in Figure 1. It is worth noting that the diffraction patterns of the clathrate structures (Figure 1A−D) show the most significant differences in the region of 2θ between 7° and 15°. In particular, the intensities of the two sharp reflections at 2$\theta \cong 8°$ and 10° change in opposite way with the content of the toluene included in the clathrate structure. Indeed, the lower the content of toluene, the lower the intensity of the reflection at 2$\theta \cong 10°$ and the higher the intensity of the reflection at 2$\theta \cong 8°$. For the emptied clathrate form (δ_e form, including less than 1 wt % toluene) the reflection at 2$\theta \cong 10°$ is very weak (Figure 1D). Moreover, with the decrease of the content of toluene, the intensity of a broad diffraction peak centered at 2$\theta \cong 13.5°$ increases; it becomes maximum for the emptied δ form (Figure 1D).

This behavior is in qualitative agreement with structure factors calculations of reflections observed in the region of 2θ between 7° and 14° (reported in Table 1) performed for the crystal structure of the clathrate δ form including toluene, proposed by Chatani et al.[14] (monoclinic unit cell with axes $a = 17.58$ Å, $b = 13.26$ Å, $c = 7.71$ Å, and $\gamma = 121.2°$, space group $P2_1/a$), by varying the occupancy factor of the atoms of toluene. It is apparent, from Table 1, that the intensities of the 010 and 111 reflections at 2$\theta = 7.8°$ and 13.4°, respectively, increase, whereas that of the $\bar{2}10$ reflection at 2$\theta = 10.2°$ decreases, with the decrease of the occupancy factor of the atoms of toluene.

The X-ray powder diffraction patterns of Figure 1 indicate that the crystal structure of the emptied clathrate δ form is very similar to that proposed by Chatani et al.[14] for the clathrate including toluene; the differences observed in the patterns are a consequence of the gradual removal of the guest. However, we observe that the reflections located at 2$\theta = 7.9°$ and 10.2° in the profiles of the clathrate δ form (Figure 1A) are located at 2$\theta = 8.3°$ and 10.6° in the profile of the emptied δ form (Figure 1D), indicating that some change in the constants of the unit cell also occurs. It is worth noting that the diffraction patterns of the emptied δ form (Figure 1D) and the γ form (Figure 1E) are significantly different, although both include only chains of s-PS in the s(2/1)2 helical conformation, essentially without guest molecules.

X-ray Diffraction Patterns of Oriented Samples. Unit Cell of the Emptied Clathrate Form. The X-ray diffraction patterns of oriented samples of clathrate δ forms, containing toluene and chloroform, are reported in Figures 2A and 3A, respectively. The X-ray diffraction patterns of the corresponding oriented emptied samples (obtained by extraction of the clathrate fibers with boiling acetone) are reported in Figures 2B and 3B, respectively. The patterns of clathrate δ forms of Figures 2A and 3A are slightly different since the intensities and the precise locations of the reflections are variable with the kind and the amount of the guest.[1,2] The patterns of the emptied samples of Figures 2B and 3B are, instead, very similar, and hence they can be assumed as the pattern of the emptied clathrate δ form (δ_e form).

The reflections observed in the X-ray diffraction pattern of Figure 2A are accounted for by the monoclinic unit cell with axes $a = 17.58$ Å, $b = 13.26$ Å, $c = 7.71$ Å, and $\gamma = 121.2°$ proposed by Chatani et al.[14] for the clathrate δ form including toluene. The reflections observed in the X-ray diffraction pattern of the emptied clathrate δ form of Figure 2B are reported in Table 2. The reflections are accounted for by a monoclinic unit cell with axes $a = 17.4$ Å, $b = 11.85$ Å, $c = 7.70$ Å, and $\gamma = 117°$. The calculated density is 0.977 g/cm^3 with four chains of s-PS in helical s(2/1)2 conformation included in the unit cell. This is in agreement with the experimental density of 1.04 g/cm^3, which is lower than the density of amorphous s-PS (1.055 g/cm^3). The space group is $P2_1/a$, in accordance with the absence of $hk0$ reflections with $h = 2n + 1$.

As already observed for the powder diffraction profiles of Figure 1, the most relevant differences between the X-ray fiber diffraction patterns of the clathrate δ form of Figure 2A and the emptied δ form of Figure 2B are the intensities of the two equatorial reflections in the low-2θ region, corresponding to 010 and $\bar{2}10$ reflections, and the intensity of the diffraction spot at 2$\theta = 13.4°$ on the first layer line (corresponding to 101 and $\bar{1}11$ reflections). Indeed, the $\bar{2}10$ reflection at 2$\theta = 10.6°$ is very weak for the emptied δ form (Figure 2B), whereas it is strong (at 2$\theta = 10.2°$) for the clathrate δ form (Figure 2A); the intensity of the $\bar{1}11$ reflection at 2$\theta =$ 13.4 is strong for the emptied δ form (Figure 2B), while it is weak for the clathrate δ form (Figure 2A). The 101 reflection is absent in the clathrate δ form, whereas it has a strong intensity in the emptied δ form. As observed before, this behavior is in agreement with the calculations of Table 1.

Packing of the Chains in the Emptied Clathrate Form. The structural model for the emptied δ form was refined by performing packing energy calculations. The

Table 3. Results of the Minimization of the Packing Energy

	a (Å)	*b* (Å)	*c* (Å)	γ (deg)	*E* (kJ/mol, mu)
model of Chatani of Figure 5 without the molecules of toluene with *a*, *b*, and γ constant	17.58	13.26	7.71	121.2	−19.9
model of Chatani of Figure 5 without the molecules of toluene with *a*, *b*, and γ variable	17.2	11.73	7.71	116.8	−24.3
model of the emptied δ form (δ_e form) of Figure 4	17.4	11.85	7.70	117.0	−23.85

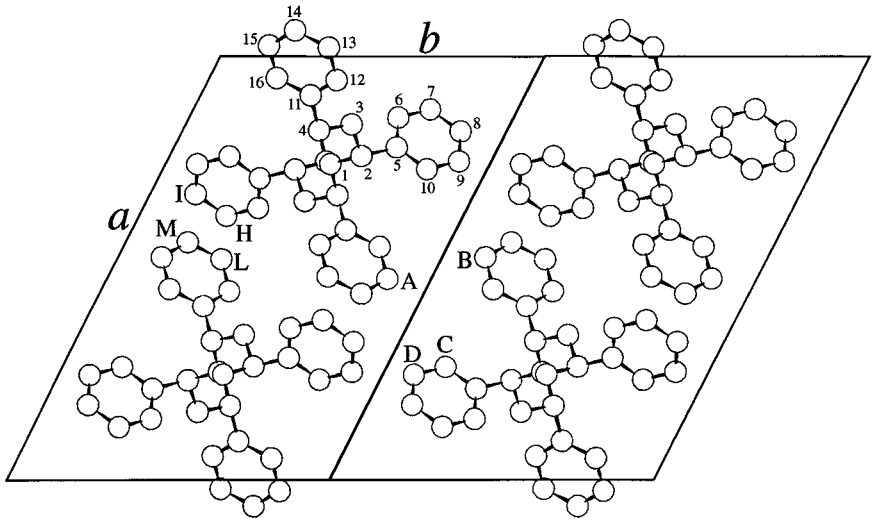

Figure 4. Model of packing for the crystal structure of the emptied δ form of s-PS (δ_e form) in the space group $P2_1/a$. Two cells along b are reported. The carbon atoms of the asymmetric unit are labeled with the numbers 1−16. The carbon atoms which give the lowest intermolecular contact distances between and inside ac layers of macromolecules are labeled with the letters A−D, H−M. The values of the contact distances are reported in Table 4.

Table 4. Lowest Intermolecular Distances between Phenyl Carbon Atoms of s-PS Chains in the Models of Crystal Structures of the Clathrate δ Form Including Toluene[14] of Figure 5 and the Emptied Clathrate δ Form of Figure 4

clathrate δ form (Figure 5)		emptied clathrate δ form (δ_e form, Figure 4)	
A−B	4.4 Å	A−B	3.7 Å
A−C	4.3 Å	A−C	3.9 Å
A−D	4.2 Å	A−D	3.7 Å
E−F	4.0 Å	H−L	4.0 Å
E−G	3.9 Å	I−M	4.1 Å
H−G	3.9 Å		

conformation of the chain (and hence the c axis) has been kept constant in the calculations. The values of the conformational parameters were obtained performing minimizations of the internal energy by using the potential functions and the method described in ref 19. At variance with calculations of ref 19, in these minimizations we have varied independently the bond angles of two adjacent methylene carbon atoms. The obtained chain conformation is very similar to that deduced from the data reported by Chatani et al.[14] The bond angle on the methine carbon atoms is 111.8°, whereas those on the two methylene carbon atoms belonging to two successive monomeric units are 115.8° and 116.8°; the two torsion angles, for the s(2/1)2 helical symmetry, are 180.1° and 63.2°.

The packing energy calculations have been performed using the same nonbonded energy functions used in the minimizations of the conformational energy. The chain axis has been positioned at $x/a = 0.25$, $y/b = 0.5$ (corresponding to the position of the 2_1 axis in the space group $P2_1/a$); during the minimizations, the orientation of the chain around the 2-fold screw axis and the height of the chain along z were varied.

The results of the minimization of the packing energy for our model of the emptied δ form, in comparison with the calculations performed on the structural model of Chatani et al.,[14] for the clathrate δ form without the

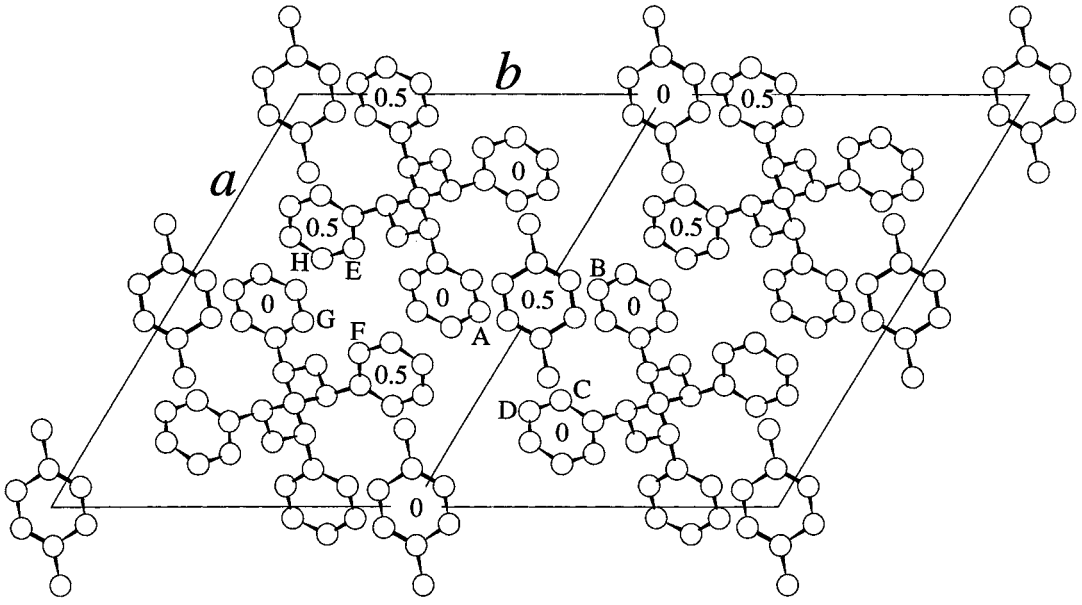

Figure 5. Model of packing, in the space group $P2_1/a$, for the crystal structure of the clathrate δ form of s-PS including toluene proposed by Chatani et al.[14] Two cells along b are reported. The methyl carbons of the molecules of toluene are shown in the two statistical *para* positions having occupancy factor 0.5.[14] The approximate fractional coordinates of the heights of the barycenters of the phenyl rings are also shown. The carbon atoms which give the lowest intermolecular contact distances between and inside ac layers of macromolecules are labeled with the letters A−H. The values of the contact distances are reported in Table 4.

Table 5. Fractional Coordinates of the Carbon Atoms of the Asymmetric Unit in the Model of Figure 4 for the Emptied Clathrate Form of s-PS (δ_e Form) in the Space Group $P2_1/a$[a]

	x/a	*y/b*	*z/c*
1	0.253	0.508	0.012
2	0.234	0.591	0.140
3	0.159	0.512	0.262
4	0.173	0.421	0.384
5	0.213	0.686	0.045
6	0.143	0.644	−0.066
7	0.124	0.731	−0.153
8	0.176	0.860	−0.129
9	0.246	0.902	−0.018
10	0.265	0.815	0.069
11	0.091	0.340	0.481
12	0.055	0.396	0.592
13	−0.021	0.322	0.681
14	−0.061	0.191	0.658
15	−0.026	0.135	0.547
16	0.050	0.209	0.458

[a] The asymmetric unit corresponds to the two monomeric units labeled in Figure 4.

molecules of toluene, are reported in Table 3. For the latter model, the energy has been minimized with the parameters of the Chatani unit cell kept constant, as well as by changing the parameters *a*, *b*, and γ of the cell, the orientation of the chain around the chain axis, and its height along *z*.

It is apparent, from Table 3, that, removing the molecules of toluene from the unit cell of Chatani,[14] a shortening of the *b* axis from 13.26 to 11.73 Å and a lowering of the value of γ from 121.2° to 116.8° occur, while the *a* axis remains practically unaltered. The distance $b \sin \gamma$ between *ac* layers of macromolecules is shortened from 11.34 to 10.47 Å. The values of the parameters of the unit cell foreseen from the minimization of the packing energy are very similar to the experimental values found by us for the emptied δ form ($b \sin \gamma = 10.56$ Å). The values of the packing energy for the experimental unit cell and the minimized unit cell are practically coincident (Table 3). It is, however, worth noting that the employed minimization technique allows to find local energy minima, and the absolute minimum may also be different.

A model for the crystal structure of the emptied δ form, in the space group $P2_1/a$, is reported in Figure 4; the model of Chatani et al.,[14] for the clathrate δ form including molecules of toluene, is reported for comparison in Figure 5. The lowest intermolecular atomic distances between phenyl carbon atoms of s-PS chains in the models of Figures 4 and 5 are reported in Table 4. It is apparent, from Figure 5 and Table 4, that the

Table 6. Comparison between the Calculated Intensities (I_c) for the Model of the Emptied δ Form of Figure 4, in the Space Group $P2_1/a$, and the Experimental Intensities (I_o) Observed in the X-ray Fiber Diffraction Pattern of Figure 2B[a]

hkl	d_{obs}(Å)	d_{calc}(Å)	I_c		I_o [b]
010	10.56	10.56	570		vs
$\bar{2}10$	8.34	8.300	3		vw
200	7.69	7.752	124		vw
$\bar{2}20$	5.91	5.742	290		w
020	5.22	5.279	18	163	w
210		5.220	145		
$\bar{4}10$	4.28	4.329	47	58	w
$\bar{4}20$		4.150	11		
$\bar{2}30$		3.950	39		
400		3.876	36		
220		3.659	18		
030		3.519	20		
230		2.767	11		b
040		2.640	19		
$\bar{6}40$		2.499	13		
101	6.63	6.896	588	1414	vs
$\bar{1}11$		6.395	826		
011		6.221	23		
201		5.463	11		
111	5.28	5.304	440		ms
$\bar{1}21$		4.672	44		
$\bar{2}21$		4.603	29		
211	4.30	4.320	54	610	s
301		4.291	150		
$\bar{3}21$		4.192	230		
$\bar{4}11$	3.78	3.774	261	378	s
$\bar{4}21$		3.653	117		
131		2.906	26		
$\bar{6}21$		2.712	12		
002	3.80	3.850	88		ne
102	3.58	3.737	114	548	m
$\bar{1}12$		3.650	292		
012		3.617	8		
$\bar{2}12$		3.493	46		
202		3.448	37		
112		3.407	51		
212	3.10	3.098	8	252	mw
302		3.087	107		
$\bar{3}22$		3.050	137		
$\bar{4}12$		2.877	59		
402	2.70	2.731	37	119	vw
$\bar{3}32$		2.714	2		
$\bar{4}32$		2.598	80		
$\bar{5}12$		2.559	22		
502		2.415	22		
$\bar{4}42$		2.301	14		
512		2.192	14		
422		2.160	12		
602		2.146	17		
$\bar{6}42$		2.096	10		

[a] The Bragg distances, observed in the X-ray fiber diffraction pattern of Figure 2B and calculated for the unit cell with axes $a = 17.4$ Å, $b = 11.85$ Å, $c = 7.70$ Å, and $\gamma = 117°$, are also shown. Only the calculated intensities of not observed reflections greater than 10 are reported. [b] vs = very strong, s = strong, ms = medium strong, m = medium, mw = medium weak, w = weak, vw = very weak, ne = not evaluated.

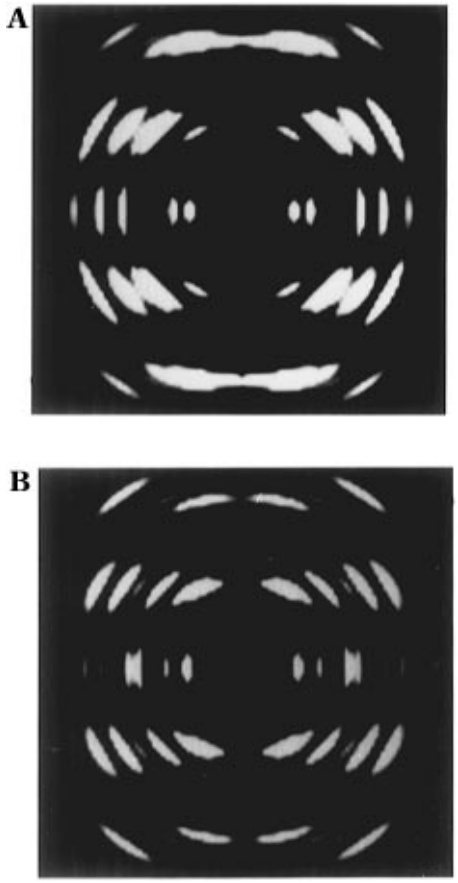

Figure 6. X-ray fiber diffraction patterns of the clathrate δ form including toluene, calculated for the model of Chatani et al.[14] (A), and the corresponding emptied clathrate δ form calculated for the model of Figure 4 (B).

intermolecular distances between carbon atoms of the polymer chains are greater than 4.2 Å, between *ac* layers of macromolecules, whereas some distances are at the limit values allowed by the van der Waals distances inside the *ac* layers of macromolecules. Moreover the shortest distance between polymer carbon atoms and toluene carbons in the model of Figure 5 is 3.47 Å, as reported by Chatani et al.[14] This indicates that, after the removal of the molecules of toluene, there is only a need to shorten slightly the *b* axis to bring the intermolecular contact distances close to the limits allowed by the sum of the van der Waals radii, as occurs in the model of Figure 4 (Table 4). The fractional coordinates of the asymmetric unit (two monomeric units) for the model of Figure 4, in the space group $P2_1/a$, are reported in Table 5.

The calculated X-ray fiber diffraction patterns for the model of Chatani et al.[14] of the clathrate δ form including toluene and for the model of Figure 4 of the emptied clathrate δ form are reported in Figure 6A,B, respectively. The differences between the X-ray diffraction patterns of the clathrate δ form and the emptied δ form, observed in the experimental patterns of Figure 2A,B, are also observed in the calculated X-ray diffraction patterns of Figure 6. Indeed the strong $\bar{2}10$ reflection in the calculated X-ray diffraction pattern of the clathrate δ form (Figure 6A) becomes very weak in the X-ray diffraction pattern of the emptied δ form (Figure 6B). Moreover the weak 101 and $\bar{1}11$ reflections for the clathrate δ form (Figure 6A) become of strong intensities in the emptied δ form (Figure 6B).

A comparison between the calculated intensities for the model of Figure 4, in the space group $P2_1/a$, and the intensities observed in the X-ray fiber diffraction pattern of the emptied δ form of Figure 2B are reported in Table 6. A good agreement is apparent.

Conclusions

The emptied clathrate δ form (δ_e form) of s-PS, including less than 1 wt % toluene, is obtained removing the guest molecules from different clathrate forms by extractions of clathrate δ form samples with boiling acetone. The emptied clathrate form of s-PS is different from the γ form which is obtained by annealing of the δ form; two different pure helical forms, free from the guest molecules (δ_e and γ forms), exist for s-PS.

The crystal structure of the emptied clathrate form has been determined by the analysis of the X-ray fiber diffraction pattern and packing energy calculations. Chains in the helical s(2/1)2 conformation are packed in the monoclinic unit cell with axes $a = 17.4$ Å, $b = 11.85$ Å, $c = 7.70$ Å, and $\gamma = 117°$ according to the space group $P2_1/a$. The structure is similar to the model proposed by Chatani et al.[14] for the crystal structure of the clathrate δ form including toluene: the *b* axis is shorter (11.85 vs 13.26 Å) and the distance $b \sin \gamma$ between *ac* layers of macromolecules is shortened from 11.34 to 10.56 Å as a consequence of the removal of the guest molecules. The differences observed in the X-ray diffraction patterns of the clathrate δ form and the emptied clathrate δ form (δ_e form) are a consequence mainly of the removal of the guest molecules.

Acknowledgment. Financial support from the Ministero dell'Università e della Ricerca Scientifica e Tecnologica is gratefully acknowledged.

References and Notes

(1) Immirzi, A.; De Candia, F.; Iannelli, P.; Vittoria, V.; Zambelli, A. *Makromol. Chem., Rapid Commun.* **1988**, *9*, 761.
(2) Guerra, G.; Vitagliano, V. M.; De Rosa, C.; Petraccone, V.; Corradini, P. *Macromolecules* **1990**, *23*, 1539.
(3) De Rosa, C.; Guerra, G.; Petraccone, V.; Corradini, P. *Polym. J.* **1991**, *23*, 1435.
(4) De Rosa, C.; Rapacciuolo, M.; Guerra, G.; Petraccone, V.; Corradini, P. *Polymer* **1992**, *33*, 1423.
(5) Rapacciuolo, M.; De Rosa, C.; Guerra, G.; Mensitieri, G.; Apicella, A.; Del Nobile, M. A. *J. Mater. Sci. Lett.* **1991,** *10*, 1084.
(6) Chatani, Y.; Shimane, Y.; Inoue, Y.; Inagaki, T.; Ishioka, T.; Ijitsu, T.; Yukinari, T. *Polymer* **1992**, *33*, 488.
(7) Greis, O.; Xu, Y.; Asano, T.; Petermann, J. *Polymer* **1989**, *30*, 590.
(8) De Rosa, C. *Macromolecules* **1996**, *29*, 8460.
(9) Chatani, Y.; Shimane, Y.; Ijitsu, T.; Yukinari, T. *Polymer* **1993**, *34*, 1625.
(10) De Candia, F.; Filho, A. R.; Vittoria, V. *Makromol. Chem., Rapid Commun.* **1991**, *12*, 295.
(11) Petraccone, V.; Auriemma, F.; Dal Poggetto, F.; De Rosa, C.; Guerra, G.; Corradini, P. *Makromol. Chem.* **1993**, *194*, 1335.
(12) Auriemma, F.; Petraccone, V.; Dal Poggetto, F.; De Rosa, C.; Guerra, G.; Manfredi, C.; Corradini, P. *Macromolecules* **1993**, *26*, 3772.
(13) Manfredi, C.; De Rosa, C.; Guerra, G.; Rapacciuolo, M.; Auriemma, F.; Corradini, P. *Macromol. Chem. Phys.* **1995**, *196*, 2795.
(14) Chatani, Y.; Shimane, Y.; Inagaki, T.; Ijitsu, T.; Yukinari, T.; Shikuma, H. *Polymer* **1993**, *34*, 1620.
(15) Chatani, Y.; Inagaki, T.; Shimane, Y.; Shikuma, H. *Polymer* **1993**, *34*, 4841.
(16) Guerra, G.; Manfredi, C.; Rapacciuolo, M.; Corradini, P.; Mensitieri, G.; Del Nobile, M. A. Italian Patent 1994 (CNR).
(17) Zambelli, A.; Pellecchia, C.; Oliva, L.; Longo, P.; Grassi, A. *Macromol. Chem.* **1991**, *192*, 223.
(18) Cromer, D. T.; Maan, J. B. *Acta Crystallogr.* **1968**, *A24*, 321.
(19) Corradini, P.; Napolitano, R.; Pirozzi, B. *Eur. Polym. J.* **1990**, *26*, 157.

MA970061Q